

Shaped Comb Fingers for Tailored Electromechanical Restoring Force

Brian D. Jensen, *Student Member, ASME*, Senol Mutlu, Sam Miller, Katsuo Kurabayashi, *Member, IEEE, Member, ASME*, and James J. Allen, *Member, ASME*

Abstract—Electrostatic comb drives are widely used in microelectromechanical devices. These comb drives often employ rectangular fingers which produce a stable, constant force output as they engage. This paper explores the use of shapes other than the common rectangular fingers. Such shaped comb fingers allow customized force-displacement response for a variety of applications. In order to simplify analysis and design of shaped fingers, a simple model is developed to predict the force generated by shaped comb fingers. This model is tested using numerical simulation on several different sample shaped comb designs. Finally, the model is further tested, and the use of shaped comb fingers is demonstrated, through the design, fabrication, and testing of tunable resonators which allow both up and down shifts of the resonant frequency. The simulation and testing results demonstrate the usefulness and accuracy of the simple model. Finally, other applications for shaped comb fingers are described, including tunable sensors, low-voltage actuators, multistable actuators, or actuators with linear voltage-displacement behavior. [879]

Index Terms—Tunable resonators, variable gap electrodes.

I. INTRODUCTION

THE COMB-DRIVE actuator is one of the main building blocks of microelectromechanical systems (MEMS). Its working principle is based on an electrostatic force that is generated between biased interdigitated conductive combs. Because of its capability of force generation or varying capacitance, it finds wide application in micro-mechanical systems. Sample applications include polysilicon microgrippers [1], scanning probe devices [2], force-balanced accelerometers [3], actuation mechanisms for rotating devices [4], laterally oscillating gyroscopes [5], and radio frequency (RF) filters [6]. Consequently, any improvement to this basic actuator could have far-reaching effects.

The most commonly used comb design consists of interdigitated rectangular fingers. These fingers exhibit constant force

output over a wide range of displacement, and they allow capacitance to vary linearly with engagement—a valuable tool in the design of many sensors and actuators. However, many applications exist for comb fingers which are not rectangular. Such fingers would allow tailoring of electromechanical response for a wide variety of applications. Specifically, in this paper, we demonstrate shaped comb finger designs with linear force-deflection profiles. This linear relationship partially compensates for the mechanical restoring force due to the action of the suspension spring, effectively weakening or stiffening the spring. A tunable resonator, with resonant frequency depending on dc voltage, results.

Several previous researchers have investigated various comb shapes. Hirano *et al.* [7] reported techniques for fabricating fingers which could dramatically reduce the separation gap after only a short motion. These fingers were designed for maximum possible force output at a nearly constant rate. Rosa *et al.* [8] continued this search for high-force actuators by designing and testing actuators with angled comb fingers. Ye *et al.* [9] studied directly the force-deflection behavior of a number of finger designs using a two-dimensional numeric electrostatic solution. They reported designs with linear, quadratic, and cubic force-engagement behavior. Ye and Mukherjee [10] extended this work by fabricating a shaped-finger comb drive; however, the lithographic resolution used in fabrication was not great; and the results proved inconclusive.

The objective of this paper is to further facilitate shaped comb finger design by introducing a simple analytical model to predict force-displacement behavior for an arbitrary finger shape. This model is validated by comparing it to three-dimensional modeling of several comb finger shapes. Further validation is carried out by using the simple model to design two further comb shapes to produce highly linear force-displacement behavior. These comb shapes allow voltage-controlled tuning of resonant frequency. These finger shapes were fabricated and tested by comparing resonant frequency measurements to predicted frequency shifts for tunable resonators. Finally, with model validation complete, further applications of shaped comb fingers are postulated.

II. COMB FINGER ANALYTICAL MODELING

A comb-drive actuator consists of moving and fixed conductive fingers. Bias voltage is applied across the fingers, generating electrostatic force. The magnitude of the force depends on the applied voltage as well as the geometry of the fingers. For rectangular comb fingers, the geometry results in a constant

Manuscript received May 25, 2002; revised October 21, 2002. This work was supported in part by a National Science Foundation Graduate Research Fellowship and a National Science Foundation CAREER Award. Sandia National Laboratories is a multiprogram laboratory operated by Sandia Corporation, a Lockheed Martin Company, for the United States Department of Energy under Contract DE-AC04-94AL85000. Subject Editor H. Fujita.

B. D. Jensen and K. Kurabayashi are with the Department of Mechanical Engineering, University of Michigan, Ann Arbor, MI 48109-2125 USA (bdjensen@umich.edu; katsuo@umich.edu).

S. Mutlu is with the Department of Electrical Engineering and Computer Science, University of Michigan, Ann Arbor, MI 48109-2125 USA (smutlu@umich.edu).

S. Miller is with MEMX, Inc., Albuquerque, NM 87109 USA (sam.miller@memx.com).

J. J. Allen is with MEMS Science and Technology, Sandia National Laboratories, Albuquerque, NM 87185 USA (jjallen@sandia.gov).

Digital Object Identifier 10.1109/JMEMS.2003.809948

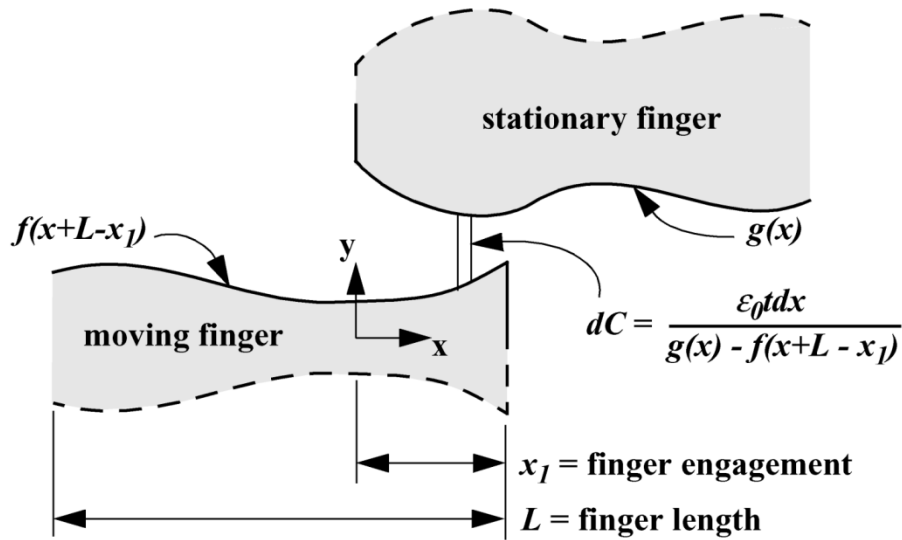


Fig. 1. Illustration of engagement of arbitrarily-shaped fingers.

gap between fixed and moving fingers as they engage. However, shaped fingers represent a way to vary the gap between the fingers. In order to find the relationship between force and gap profiles, a simple model is developed using the shaped fingers illustrated in Fig. 1. In the modeling, $f(x)$ and $g(x)$ represent the finger profiles of the moving and stationary fingers, respectively. Each function is assumed to be defined on the domain $[0, L]$, where L is the length of the fingers. Motion of the moving finger is represented by x_1 , the finger engagement, as illustrated in the figure. The force between the fingers is represented as

$$F_x = \frac{\partial E}{\partial x_1} = \frac{1}{2} V^2 \frac{dC}{dx_1} \quad (1)$$

where F_x is the electrostatic force, E is the stored energy between conductor plates, V is the applied bias, C is the capacitance between fingers, and x_1 is the relative engagement between the moving and fixed fingers, as illustrated in Fig. 1. Therefore, we can determine generated electrostatic force by calculating change in capacitance as the moving finger engages the fixed fingers. Using the parallel-plate approximation illustrated in the figure gives

$$C(x_1) = 2\epsilon_0 t \int_0^{x_1} \frac{dx}{g(x) - f(x+L-x_1)} \quad (2)$$

where t is the out-of-plane thickness of the fingers and ϵ_0 is the permittivity of free space. This equation assumes that the electrodes are substantially parallel to one another, allowing capacitance to be determined by integrating the parallel-plate formula. Hence, (2) does not apply well to piece-wise continuous functions, which have discontinuities for which (2) does not adequately predict capacitance. The factor of 2 arises because the capacitance is the same on both sides of the finger for a sym-

metrical finger shape. Furthermore, if one of the fingers is rectangular, capacitance can be approximated as

$$C = 2\epsilon_0 t \int_0^{x_1} \frac{dx}{h(x)} \quad (3)$$

where $h(x)$ is the gap profile between fingers. For example, if the moving finger is rectangular, then $f(x) = k$, where k is a constant, and $h(x) = g(x) - k$. Substitution of (3) into (1) gives

$$F_x = \frac{V^2 \epsilon_0 t}{h(x_1)}. \quad (4)$$

This is the simple model used in this paper to predict the resulting force profile of different comb shapes. Its simplicity lies in its prediction that the force acting on a shaped comb finger is simply proportional to the reciprocal of the function defining the finger shape. As stated, (4) is valid only if either the fixed or the moving finger is rectangular. For designs with both moving and fixed fingers shaped, a numerical solution is generally required, although analytical solutions are still possible for some geometries. Note also that if $h(x)$ is a constant finger gap, (4) reduces to the well-known equation for force generated by a rectangular comb finger.

III. NUMERICAL MODELING

To test the simple model developed in the preceding section, seven finger designs were modeled using the boundary element or moment method. Top views of each of the seven different designs are included in Fig. 2. Equations describing the fixed and moving finger profiles are presented in Table I. Finger design 7 is not well explained in this table because it is not described by a simple equation; rather, it is a sawtooth design with tooth pitch of $3 \mu\text{m}$ and height of $2 \mu\text{m}$ for both the moving and fixed fin-

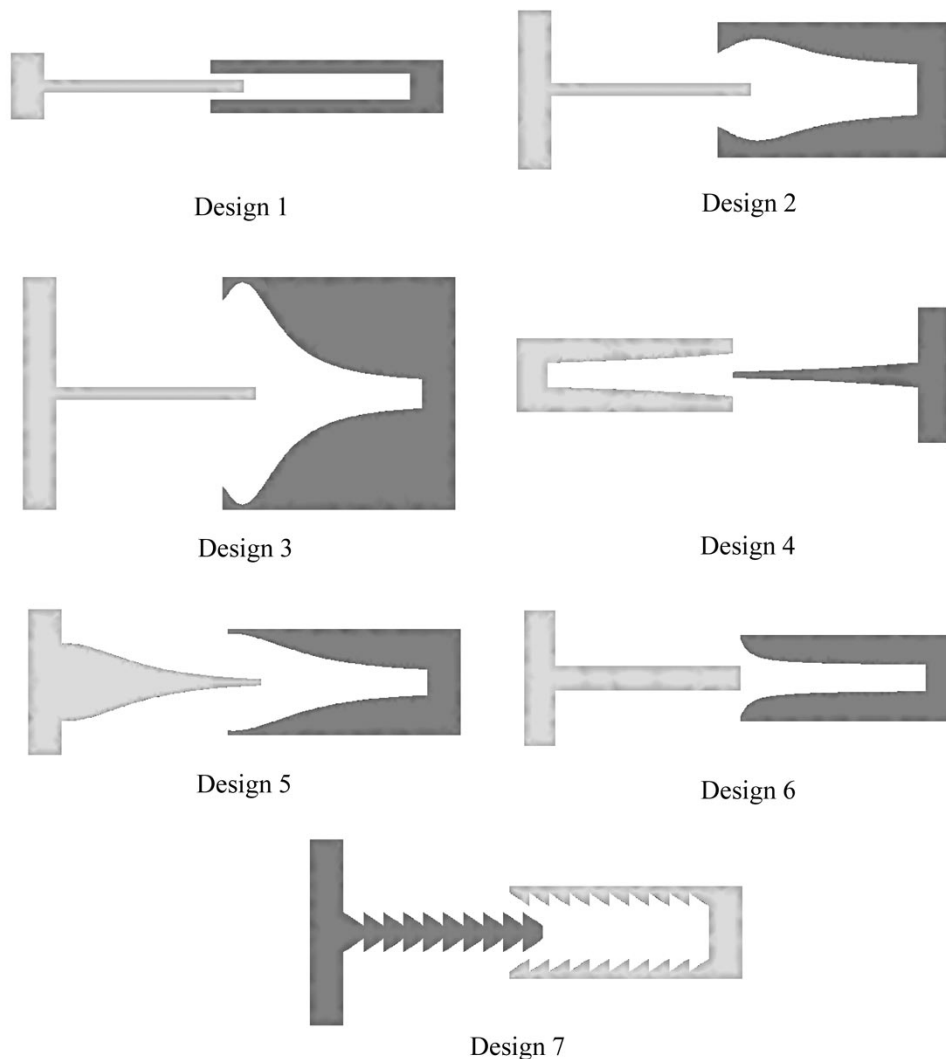


Fig. 2. The seven comb finger designs studied.

gers. The fingers for design 7 are arranged so that the minimum gap between them as they engage is $1 \mu\text{m}$. This finger design tests the accuracy of the model when applied to discontinuous functions.

The first comb finger design is the simple rectangular comb finger with a constant gap of $1 \mu\text{m}$. This design was chosen to verify that a constant force relationship resulted. The next four finger designs, number 2, 3, 4, and 5, were derived from the earlier work by Ye *et al.* [9]. They reported that designs 2 and 4 showed linear force-engagement behavior, while designs 3 and 5 were cubic. We studied these finger designs to allow a comparison with the previous work. Unfortunately, however, the description of the comb finger designs in the cited work were not clear enough to exactly duplicate either their finger designs or their results; however, the general trend in the results was examined. Finger design 6 was proposed by us to give a higher force output and slope of the linear trend than the earlier designs. Finally, we investigated design 7 to test the model's application to discontinuous functions, as previously stated.

Each finger design was modeled using a boundary element model (BEM) in CoventorWare, formerly known as MEMCAD.

The BEM simulated the capacitance of the fingers. By offsetting the mesh of the moving finger by a small amount, the derivative of capacitance with respect to engagement was estimated using the central difference equation (using a mesh offset of $0.01 \mu\text{m}$ on either side of the desired engagement). Electrostatic force was then calculated using (1). Out-of-plane thickness of all of the fingers was $4 \mu\text{m}$, and the length of fixed and moving fingers was $30 \mu\text{m}$ for all designs. In addition, the thickness of the sacrificial layer, which determines the height of the fingers above the substrate, was $2.5 \mu\text{m}$. Fig. 4 shows an isotropic view of the rectangular comb fingers used in this study. All of the simulations were performed at 1.0 V . However, it is assumed that the force output on the fingers acts as the voltage squared, so that the results may be generalized to any applied bias.

Before modeling each of the seven comb fingers, we performed a simple mesh refinement study. The boundary element mesh consisted of triangular elements covering the surface of the fingers and the substrate. The mesh was automatically generated using CoventorWare's tools. The rectangular comb fingers were simulated using a wide variety of mesh parameters, which produced a large range in the number of elements in each

TABLE I
FIXED AND MOVING FINGER PROFILES FOR DESIGNS 2–7. UNLESS OTHERWISE NOTED, THE DOMAIN FOR ALL EQUATIONS IS $x = [-25, 5]$
AND THE X-AXIS LIES ALONG THE CENTERLINE OF THE MOVING FINGER

Fixed Finger Profile	
Design#2	$g(x) = \frac{1}{0.1507 + 0.3135 \times 10^{-2}x + 0.1679 \times 10^{-2}x^2 + 0.8051 \times 10^{-4}x^3 + 0.1244 \times 10^{-5}x^4} + 1.0$
Design#3	$g(x) = \frac{1}{0.06897 - 0.5754 \times 10^{-2}x + 0.1419 \times 10^{-2}x^2 + 0.1411 \times 10^{-4}x^3 - 0.1879 \times 10^{-6}x^4} + 1$
Design#4	$g(x) = \frac{1}{0.3188 - 7246 \times 10^{-2}x}$
Design#5	$g(x) = \frac{1}{0.1522 - 0.7262 \times 10^{-2}x + 0.7469 \times 10^{-3}x^2 + 0.1893 \times 10^{-4}x^3}$
Design#6	$g(x) = \frac{6.5}{1.5 + x} + 2$
Design#7	$g(x) = 4 + \frac{2}{3} \times x \quad 0 \leq x \leq 3$
Moving Finger Profile	
Design#2	$f(x)=1$
Design#3	$f(x)=1$
Design#4	$f(x) = \frac{1}{0.3188 - 7246 \times 10^{-2}x} - 1.5$
Design#5	$f(x) = \frac{1}{0.1522 - 0.7262 \times 10^{-2}x + 0.7469 \times 10^{-3}x^2 + 0.1893 \times 10^{-4}x^3} - 1.48$
Design#6	$f(x)=2$
Design#7	$f(x) = 1 + \frac{2}{3} \times x \quad 0 \leq x \leq 3$

mesh. The electrostatic force acting on the moving finger was simulated for each mesh. Fig. 3 shows the percent difference in the predicted force compared to that predicted by the finest mesh (51,246 elements). Based on these results, the meshing parameters were chosen to match those used to generate the circled data point. This point offered a reasonable trade-off in terms of accuracy (1.1% difference) and simulation time. Each of the other finger designs was meshed using these same parameters. We assume that these parameters will perform well for the other finger shapes because their size is similar to that of the rectangular finger.

Finally, several simulations were completed to compare the force acting on one finger to that acting on a bank of comb fingers. Banks of one, two, three, four, six, and ten rectangular comb fingers were simulated. The force predicted by the simulation remained within 0.2% of the force predicted by multiplying the single-finger result with the number of fingers. Therefore, we conclude that the simulation of one finger may be generalized to a bank of any number of fingers.

A. Modeling Results

Fig. 4 shows the simulation results and simple model for design 1, the rectangular comb fingers. For the simple model, the thickness used was 15% larger than the nominal thickness (4 μm) to account for fringing fields. This fringing field correction is predicted by the approximate solution for fields around rectangular comb fingers derived in a previous work [11]. As expected, the boundary element simulation predicts a nearly constant force output over the range of engagement. The simple model predicts a constant force of 40.7 pN, which lies just above the majority of the numerical data. The mean force predicted by the numerical simulation is 39.8 pN, a difference of 2.3% from the analytical model. These results show that the data trend predicted by BEM matches the analytical equation well, with both predicting constant force at nearly the same magnitude.

Graphs showing the response for each design are plotted in Fig. 5. In these graphs, the results from the simple model accompany the BEM data. For all designs, the simple model assumed

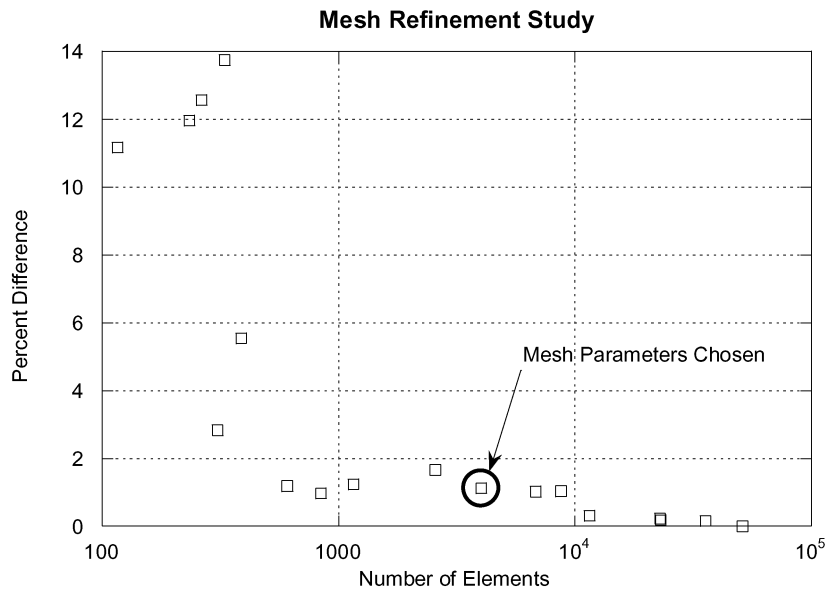
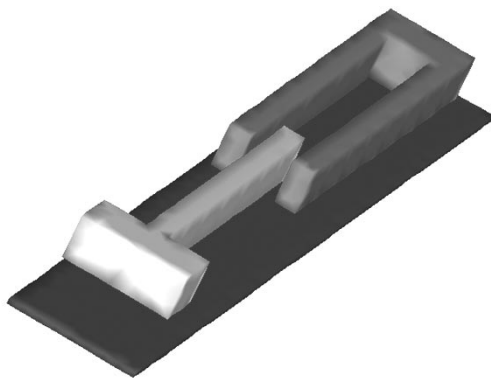
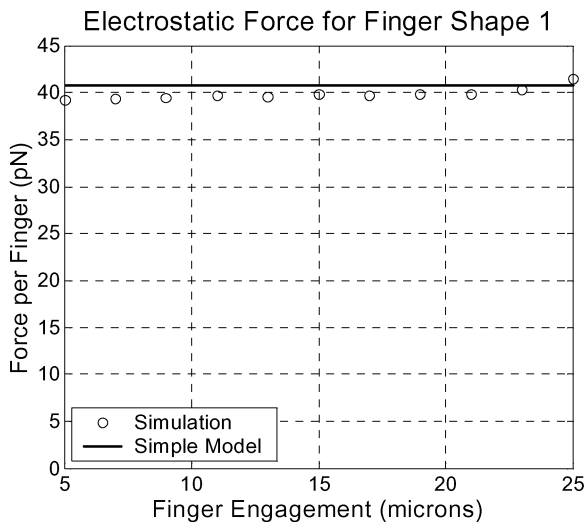


Fig. 3. Results of the mesh refinement study.



(a)



(b)

Fig. 4. Isotropic view of the numerical model of the rectangular comb fingers, and modeling results comparing the simple analytical model and numerical modeling.

10% additional thickness to account for fringing fields. While the previous study [11] does not calculate force on a curved finger, a 10% correction factor is a fairly representative value based on the equations derived in [11]. To find this representative value, we evaluated fingers of height $4 \mu\text{m}$, width $2\text{--}4 \mu\text{m}$, gap $0.5\text{--}10 \mu\text{m}$, and separation from the substrate $2.5 \mu\text{m}$. For finger designs 1, 2, 3, and 6, (4) was used to calculate the simple model curve. For design 7, we solved (2) and substituted the results into (1) to create the simple model prediction. However, for designs 4 and 5, the relationships of the two shaped fingers moving with respect to each other make derivation of an analytical equation tedious. Instead, a solution was used which numerically integrated (2) and substituted the results into (1).

The results for all finger shapes show that the BEM results follow the trend of the simple model, and the values are nearly the same for most designs. Hence, the numerical modeling results give confidence in the use of the simple model. Based on these results, we proceed to apply the simple model to design.

IV. SHAPED FINGER DESIGN IN A TUNABLE RESONATOR

As an example application of shaped comb fingers, we have designed and tested tunable micromechanical resonators using shaped fingers to achieve a resonance shift. Equation (4) allows finger shapes to be designed to give very linear force-displacement behavior over a wide range of displacement, as seen in finger shape 6. This linear response allows such fingers to be used in tunable resonators. Previously, researchers have demonstrated frequency tuning of mechanical resonators using a variety of techniques, including postprocessing deposition of material [12], postprocessing annealing [13], stiffness variation using thermal stress [14], [15], and a variety of electrostatic techniques [16]–[18]. Note that the first two methods cause a permanent resonant frequency shift, while methods based on thermal stress or electrostatic effects allow a dynamically variable resonant frequency shift. Any of these techniques allow

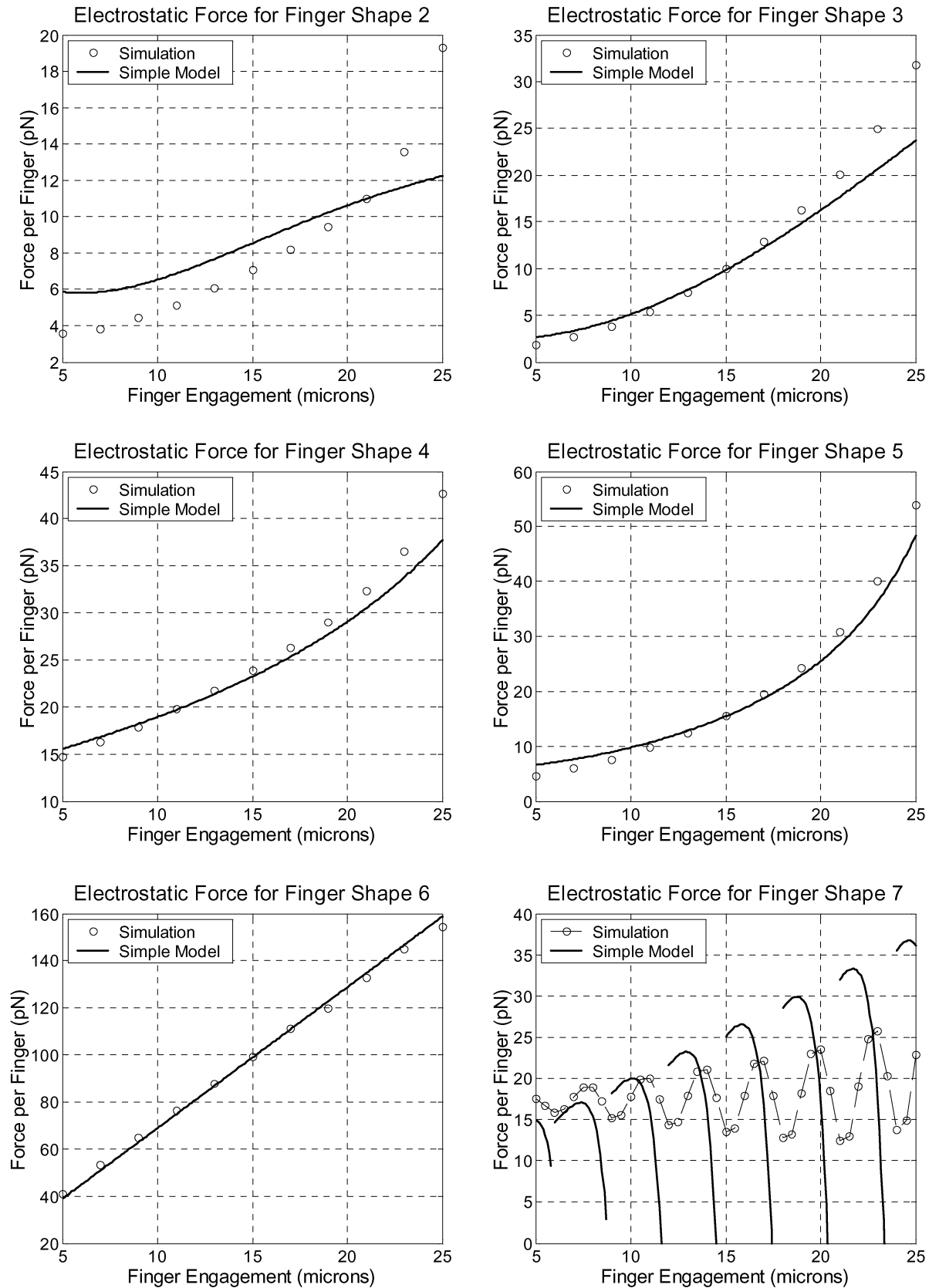


Fig. 5. Graphs showing force acting on a single finger for each of the shaped fingers. BEM results and the predictions of the simple model are shown.

correction of frequency shifts due to process variation; the dynamic techniques further allow correction of frequency shifts due to temperature change [16], [19]. Frequency tuning has also

been employed to allow matching of the drive and sense modes in gyroscopes based on the Coriolis effect [5], and electrostatic stiffness tuning has been demonstrated to improve the resolu-

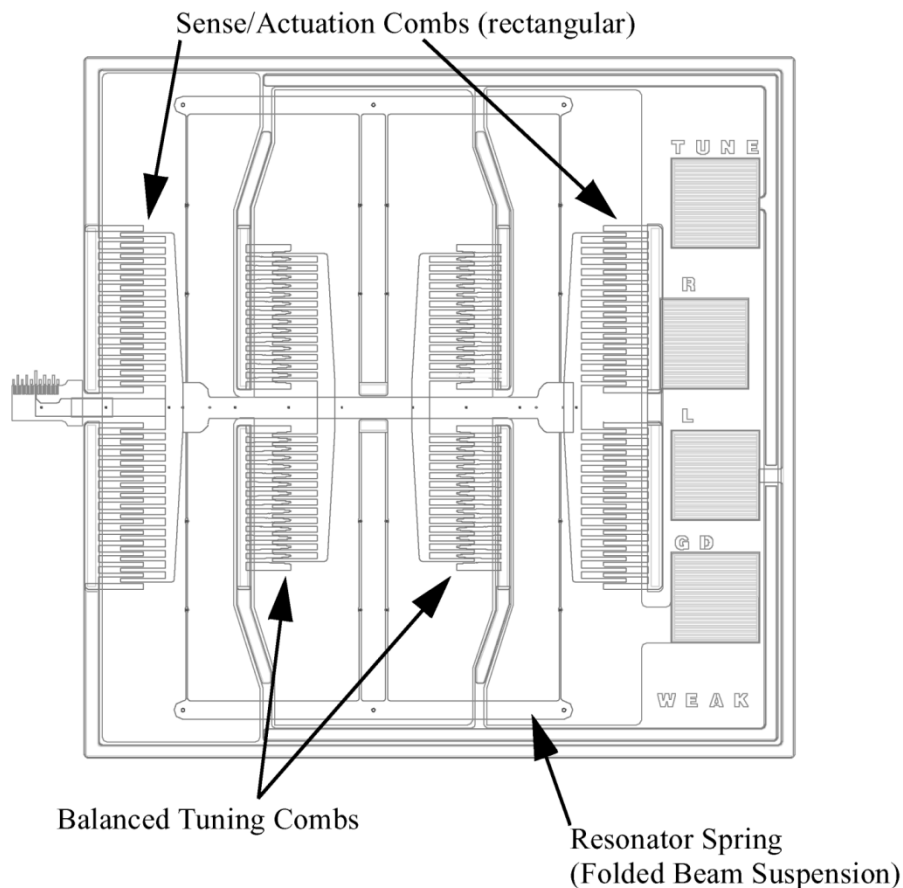


Fig. 6. Sample layout of a tunable resonator.

tion of a MEMS accelerometer [20]. Using shaped fingers, it is possible to dynamically tune resonant frequency over a large range. Large tuning ranges may allow tunable resonant sensors with active frequency control to improve sensor resolution or bandwidth, as well as tunable micromechanical filters with controllable center frequency.

A tunable resonator is created using shaped comb fingers by modifying a standard comb resonator to include one or more banks of shaped comb electrodes whose potential can be controlled independently of the drive and sense electrodes. The shaped comb finger banks are designed to give a linear force-displacement response under constant bias. Hence, assuming the resonator remains within the range of linear behavior, the shaped comb fingers act as a linear electrostatic “spring” which either stiffens or weakens the total spring constant for the system. For example, the sample layout shown in Fig. 6 includes two balanced sets of tuning fingers. By balancing tuning banks in this way, the shaped fingers exert no net force on the resonator under zero displacement.

Resonant frequency is given approximately by

$$f = \frac{1}{2\pi} \sqrt{\frac{k_T}{m}} \quad (5)$$

where f is resonant frequency, k_T is the total spring constant, and m is the resonator mass. k_T is simply the sum of the mechanical spring constant k_m and the electrostatic spring con-

stant k_e . For a bank of n shaped comb fingers with dc voltage V acting across the fingers, k_e is simply $-V^2nk_t$, where k_t describes the slope of the force-displacement line for one finger at a potential of one volt. k_t is defined as positive for a shape which causes weakening of the effective spring constant. Thus, the tuned resonant frequency f_T is given by

$$f_T = \frac{1}{2\pi} \sqrt{\frac{k_m - V^2nk_t}{m}} \quad (6)$$

giving a resonant frequency shift of

$$\frac{f_T}{f_0} = \sqrt{1 - \frac{V^2nk_t}{k_m}} \quad (7)$$

where f_0 is the untuned resonant frequency (for the case when $V = 0$).

Two different comb finger shapes were designed and tested in tunable resonators. A model of each finger shape is shown in Fig. 7. The first finger shape effectively weakens the spring, while the second stiffens it. These fingers were designed for fabrication in Sandia National Laboratories’ SUMMiT micromachining process [21]. The two layers shown in the figure represent two of the layers available for micromachining. By stacking comb fingers in this way, the overall force output of each finger is considerably increased due to the action of fringing fields between the layered fingers. The lower layer is $2.5 \mu\text{m}$ thick, the

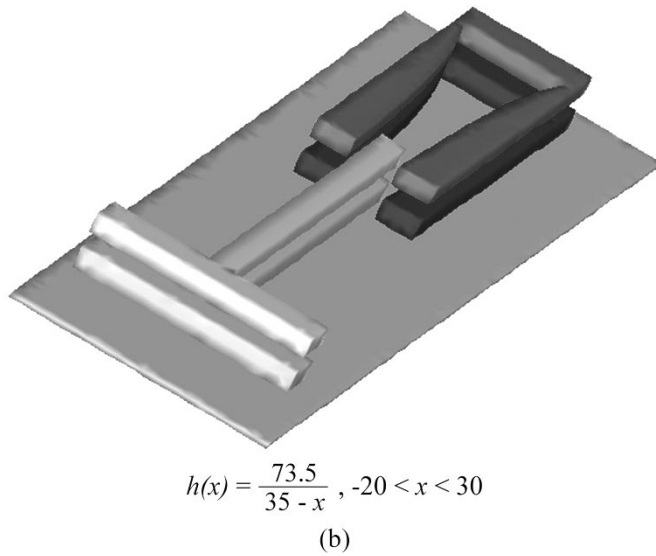
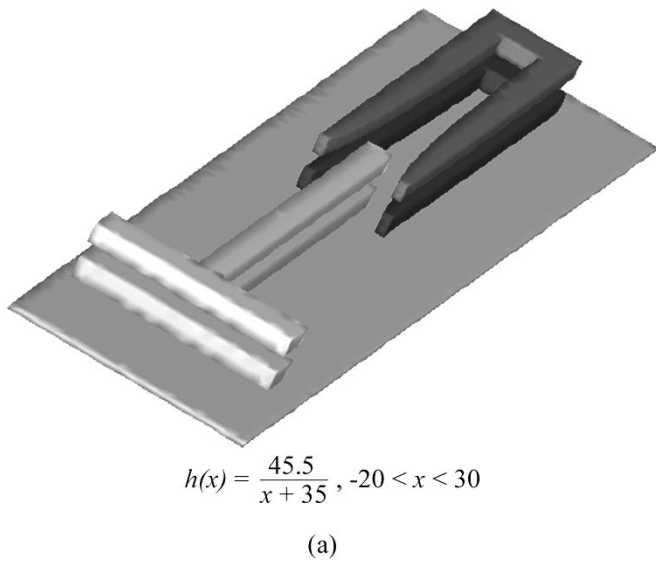


Fig. 7. Models of each shaped comb design, where (a) is the weakening finger and (b) is the stiffening finger.

upper layer is $2.25 \mu\text{m}$ thick, and they are separated by a space of $2 \mu\text{m}$. The separation between the substrate and the first layer is also $2 \mu\text{m}$. The equation describing each finger shape is given in the figure. Because one finger in each case is rectangular, $h(x)$, the gap between the fingers, is defined.

Using CoventorWare, the force acting on each of the moving fingers as a function of finger engagement was simulated. The results of each simulation are compared to the prediction of the analytical model in Fig. 8. In these graphs, the thickness t from (4) was assumed to be $6 \mu\text{m}$. While the previous work [11] does not apply to such double-layered fingers, the authors' experience has shown that this is an accurate way to model the equivalent thickness of the stacked comb finger structure, including fringing fields. For each finger, the analytical model shows good agreement with the numerical results, and the slope of the response remains nearly constant over a wide range of finger engagement. This is important in maintaining linearity during resonator operation.

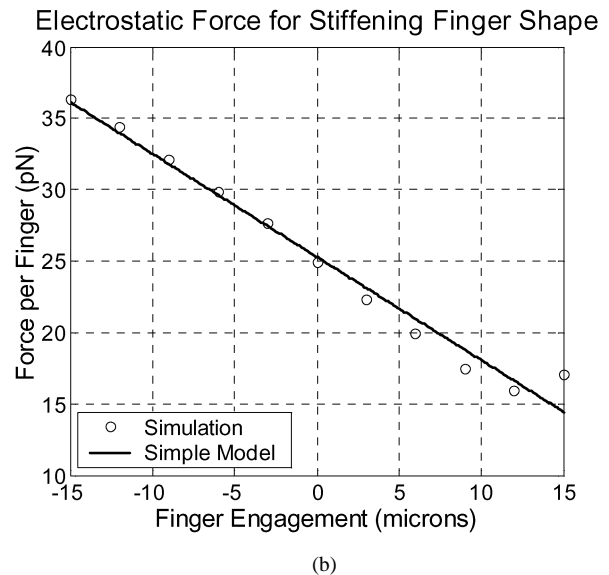
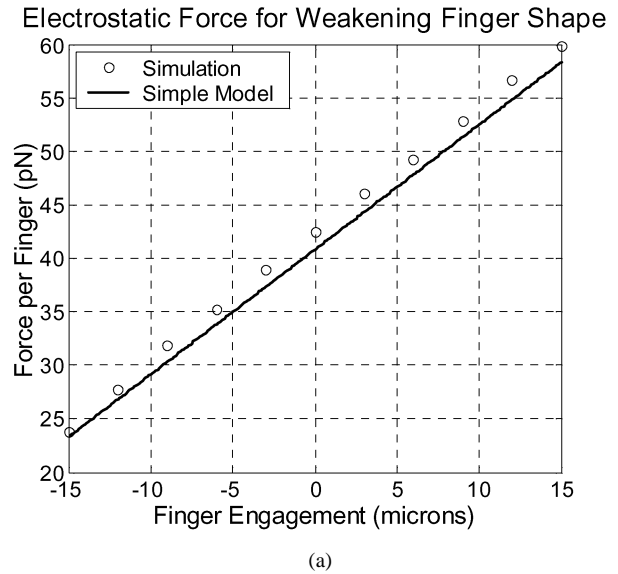
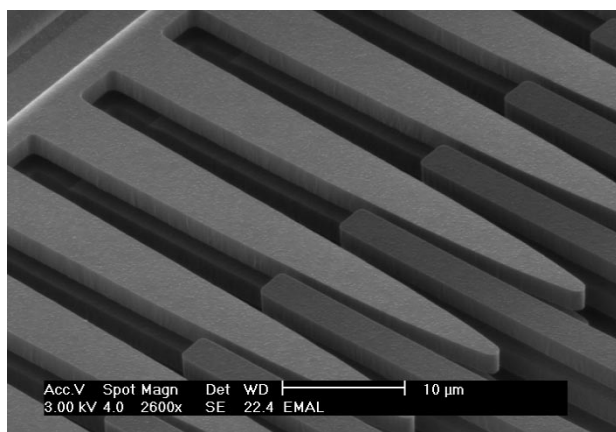
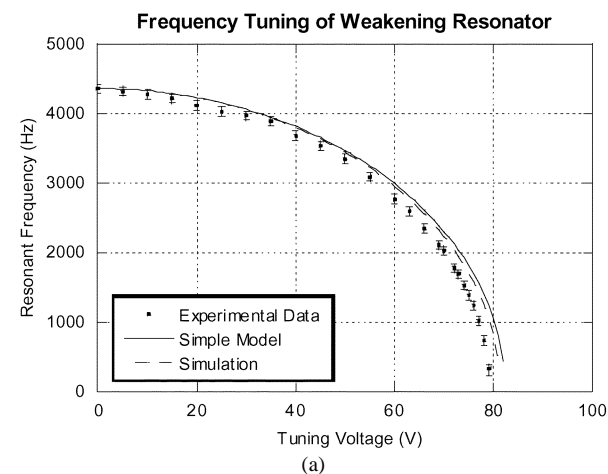


Fig. 8. Modeling results for weakening and stiffening designs.

V. FABRICATION AND TESTING

Tunable resonators incorporating the shaped fingers shown in Fig. 7 were fabricated at Sandia National Laboratories using the SUMMIT polysilicon micromachining process. In this process, the effective mask resolution is 50 nm , which allows very accurate reproduction of the function shape desired. The shaped fingers were drawn by approximating the function by a series of line segments, with the maximum error between any line segment and the desired function being 1 nm . Approximate process bias of 15 nm was accounted for by offsetting the desired function shape, though the larger mask resolution probably obscures this small offset. The tunable resonators were designed for demonstration and validation rather than any particular application. The untuned resonant frequency of the devices as designed was predicted to be about 4.3 kHz .

Released resonators were tested using the "blur envelope" technique. As the amplitude of resonator motion changes with frequency, it can be seen under a microscope as a blurring of the resonator. At large amplitude, such as occurs near resonance,



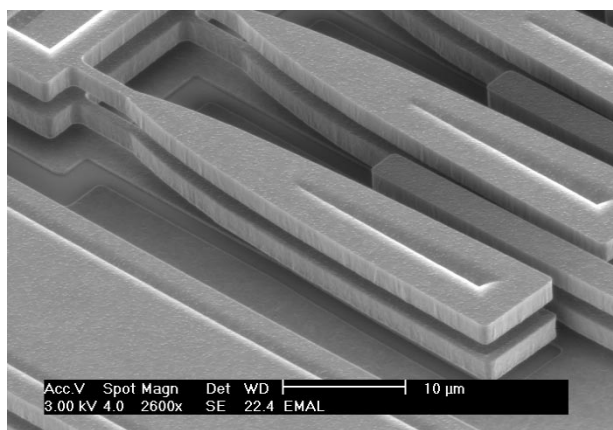
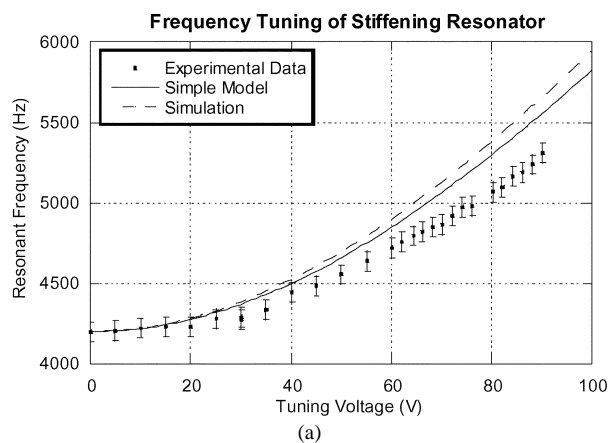
(b)

Fig. 9. Experimental results and SEM image of the weakening fingers.

the total size of the blur envelope becomes quite large, allowing simple determination of resonant frequency. In this way, the resonant frequency of the resonators was measured for varying values of the dc tuning voltage. The dc tuning voltage was supplied by a high-voltage power supply, and a function generator was used for the actuation signal, which was a sine wave with up to 10 V amplitude and up to 10 V dc offset. The amplitude and offset of the signal were decreased for high tuning voltage of the weakening resonator to keep the resonant amplitude within the usable range. The maximum amplitude of resonator vibration varied as the effective stiffness changed, but it remained below 10 μm for all tests, so that it was well within the predicted linear range of the tuning fingers.

The experimental results are shown in Fig. 9 for the weakening resonator, along with a SEM image of the weakening fingers. Fig. 10 shows the results for the stiffening resonator. In the SEM images, the finger shapes are quite smooth, so that the mask resolution seems sufficient in faithfully representing the desired functions.

As desired, the resonant frequency of each device shifts with tuning voltage. For the weakening resonator, tuning from 4.2 kHz to near 0 kHz is possible. When the resonant frequency is very low, the large voltage on the tuning fingers creates high transverse forces, causing the tuning fingers to crash together and vaporize. Thus, the lowest stable resonant frequency actually measured was 165 Hz at a tuning voltage of 79.1 V. For the



(b)

Fig. 10. Experimental results and SEM image of the stiffening fingers.

stiffening resonator, the tuning range was 4.2 kHz to 5.3 kHz. Again, the high voltage on the tuning fingers at high resonant frequencies causes the tuning fingers to crash and vaporize. 5.3 kHz (at 90.2 V) was the largest stable resonant frequency measured. Note also that most other frequency tuning methods allow only a downward shift in resonant frequency, while the use of shaped comb fingers allows either up or down frequency shifts.

The results for the weakening finger follow the predictions of the analytical model well, indicating that the simple model is appropriate for use in design. However, the stiffening resonator results show less tuning capability than predicted, though the difference is not large. The error in the analytical model is never more than 5.1% over the whole tuning range of the stiffening device.

For some applications, the stiffness change during tuning is more important than the frequency shift. Fig. 11 shows the resonator stiffness calculated from the simple model and from the experimental data using (5). For the weakening resonator, stiffness was reduced from 0.47 N/m to 0 N/m for a tuning voltage up to 80 V. For the stiffening resonator, stiffness was increased from 0.47 N/m to 0.75 N/m for a tuning voltage up to 90 V, an increase of 60%.

Therefore, the experimental results show that the simple analytical model performs well. Because of its simplicity, it is very easy to use for both design and analysis of shaped fingers. Moreover, for the tuning devices studied here, it retains approx-

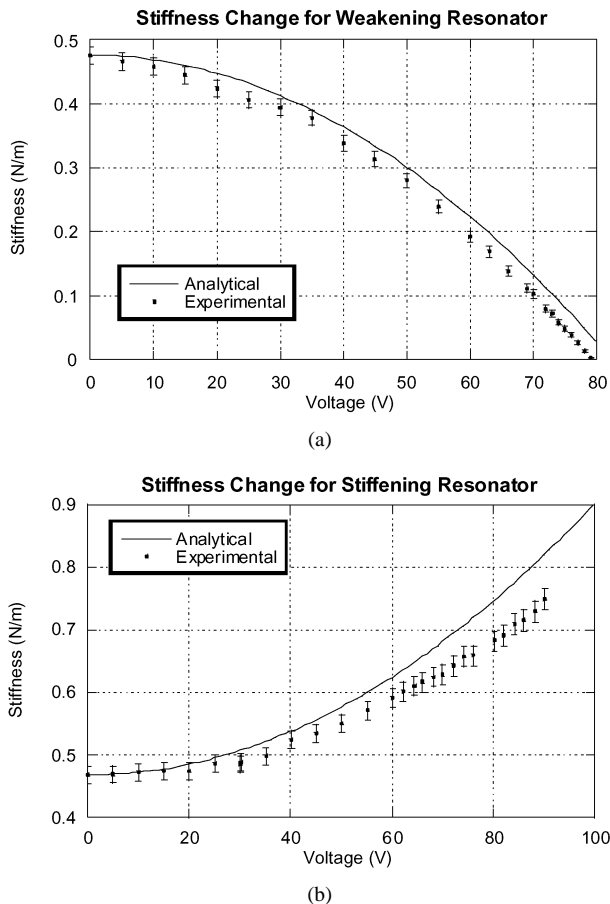


Fig. 11. Stiffness change for both resonator designs.

imately as much accuracy as more time-consuming numerical solutions.

VI. CONCLUSION

This paper has developed and validated a simple analytical model for shaped comb fingers. The model was compared to the predictions of a numerical simulation for several comb shapes, and then used in the design of two tunable resonators—in which the resonant frequency was shifted either downwards (the weakening case) or upwards (the stiffening case). Testing of the tunable resonators showed that the simple model predicted their behavior well, with both up and down frequency shifts being possible over a wide range. Another advantage of using shaped fingers for tuning is that the amplitude of the resonator is not limited to very small vibrations, with tuning possible as long as the vibration amplitude is less than the length of the engaged section of the fingers.

While this paper demonstrated the frequency tuning of resonators, shaped comb fingers could be used in a wide variety of applications involving tailored force-deflection response. For example, shaped fingers could be used to create linear voltage-displacement behavior for an actuator, so that the control system for the actuator could be simplified. An actuator could also be designed which uses shaped comb fingers to create multiple stable positions in its motion. Fingers with a linear response, like those demonstrated in this paper, could also be used to decrease the effective stiffness of an actuator carrying

a load, which would reduce both the time-varying voltage component and the power dissipation for the actuator. Linear force-displacement fingers could also allow in-plane parametric resonators, which have been suggested for use in high-resolution mass sensors [22]. Shaped fingers also allow the design of accelerometers which could operate at a wide range of spring stiffness. High stiffness would allow low-resolution operation with high bandwidth, while low stiffness would be useful for high-resolution operation with reduced bandwidth. The ability to use the same accelerometer package for such a wide variety of measurements could decrease fabrication costs by reducing the need for design and manufacture of multiple sensors.

ACKNOWLEDGMENT

The assistance of M. Yu in gathering experimental data is gratefully acknowledged. The staff of the Microelectronics Development Laboratory at Sandia National Laboratories are also gratefully acknowledged for their fabrication work.

REFERENCES

- [1] C.-J. Kim, A. P. Pisano, R. S. Muller, and M. G. Lim, "Polysilicon microgripper," in *IEEE Solid-State Sensor and Actuators Workshop*, Hilton Head, SC, June 1990, pp. 48–51.
- [2] J. J. Yao, S. C. Arney, and N. C. MacDonald, "Fabrication of high frequency two-dimensional nanoactuators for scanned probe devices," *Proc. IEEE MEMS*, pp. 14–22, 1992.
- [3] W. Yun, R. T. Howe, and P. R. Gray, "Surface micromachined digitally force balanced accelerometer with integrated CMOS detection circuitry," in *IEEE Solid-State Sensor and Actuators Workshop*, Hilton Head, SC, June 1992, pp. 126–131.
- [4] J. J. Sniegowski and E. J. Garcia, "Surface-micromachined gear trains driven by an on-chip electrostatic micro-engine," *IEEE Electron. Device Lett.*, pp. 366–368, 1996.
- [5] K.-Y. Park, C.-W. Lee, Y.-S. Oh, and Y.-H. Cho, "Laterally oscillated and force-balanced micro vibratory rate gyroscope supported by fish-hook-shaped springs," *Sensors and Actuators A*, vol. 64, pp. 69–76, 1998.
- [6] K. Wang and C. T.-C. Nguyen, "High-order medium frequency micro-mechanical electronic filters," *J. Microelectromech. Syst.*, vol. 8, pp. 534–557, 1999.
- [7] T. Hirano, T. Furuhashi, K. J. Gabriel, and H. Fujita, "Design, fabrication, and operation of submicron gap comb-drive microactuators," *J. Microelectromech. Syst.*, vol. 1, pp. 52–59, 1992.
- [8] M. A. Rosa, S. Dimitrijevic, and H. B. Harrison, "Improved operation of microelectromechanical comb-drive actuators through the use of a new angled comb finger design," in *SPIE Conf. on Smart Materials, Structures, and MEMS*, vol. 3242, 1997, pp. 212–218.
- [9] W. Ye, S. Mukherjee, and N. C. MacDonald, "Optimal shape design of an electrostatic comb drive in microelectromechanical systems," *J. Microelectromech. Syst.*, vol. 7, pp. 16–26, 1998.
- [10] W. Ye and S. Mukherjee, "Design and fabrication of an electrostatic variable gap comb drive in micro-electro-mechanical systems," *ASME Micro-Electro-Mechanical Systems (MEMS) 1998*, vol. 66, pp. 537–544, 1998.
- [11] W. A. Johnson and L. K. Warne, "Electrophysics of micromechanical comb actuators," *J. Microelectromech. Syst.*, vol. 4, pp. 49–59, 1995.
- [12] D. Joachim and L. Lin, "Selective polysilicon deposition for frequency tuning of MEMS resonators," in *15th IEEE Conference on Micro Electro Mechanical Systems*, 2002, pp. 727–730.
- [13] K. Wang, A.-C. Wong, W.-T. Hsu, and C. T.-C. Nguyen, "Frequency trimming and Q-factor enhancement of micromechanical resonators via localized filament annealing," in *1997 Int. Conf. Solid-State Sensors and Actuators*, 1997, pp. 109–112.
- [14] R. R. A. Syms, "Electrothermal frequency tuning of folded and coupled vibrating micromechanical resonators," *J. Microelectromech. Syst.*, vol. 7, no. 2, pp. 164–171, June 1998.
- [15] T. Remtma and L. Lin, "Active frequency tuning for micro resonators by localized thermal stressing effects," *Sens. Actuators, Phys. A*, vol. 91, pp. 326–332, 2001.

- [16] J. J. Yao and N. C. MacDonald, "A micromachined, single-crystal silicon, tunable resonator," *J. Micromech. Microeng.*, vol. 5, no. 3, pp. 257–264, Sept. 1995.
- [17] S. G. Adams, F. M. Bertsch, K. A. Shaw, P. G. Hartwell, N. C. MacDonald, and F. C. Moon, "Capacitance based tunable micromechanical resonators," in *Transducers '95-Proc. 8th Int. Conf. Solid-State Sensors and Actuators*, 1995, pp. 438–441.
- [18] K. B. Lee and Y.-H. Cho, "Frequency tuning of a laterally driven microresonator using an electrostatic comb array of linearly varied length," in *1997 International Conference on Solid-State Sensors and Actuators*, Chicago, IL, 1997, pp. 113–116.
- [19] K. Wang and C. T.-C. Nguyen, "High-order medium frequency micromechanical electronic filters," *J. Microelectromech. Syst.*, vol. 8, no. 4, pp. 534–557, 1999.
- [20] K.-Y. Park, C.-W. Lee, H.-S. Jang, Y. Oh, and B. Ha, "Capacitive type surface-micromachined silicon accelerometer with stiffness tuning capability," *Sens. Actuators, Phys. A*, pp. 109–116, 1999.
- [21] , <http://www.mems.sandia.gov>.
- [22] K. L. Turner, S. A. Miller, P. G. Hartwell, N. C. MacDonald, S. H. Strogatz, and S. G. Adams, "Five parametric resonances in a microelectromechanical system," *Nature*, vol. 396, pp. 149–152, Nov. 12, 1998.



Brian D. Jensen received the B.S. and M.S. degrees in mechanical engineering from Brigham Young University, Provo, UT, in 1996 and 1998, respectively. He is currently pursuing the Ph.D. degree in mechanical engineering at the University of Michigan, Ann Arbor.

Before starting his Ph.D. studies, he worked at Sandia National Laboratories, Albuquerque, NM, designing and testing MEMS devices. He has received a National Science Foundation Graduate Research Fellowship as well as a National Defense Science and Engineering Graduate Fellowship. His research interests include MEMS design and modeling.

Mr. Jensen is a Student Member of the American Society of Mechanical Engineers (ASME).



Senol Mutlu received the B.S. degree in electrical engineering from University of Southern California, Los Angeles, in May 2000. He received the M.S. degree in electrical engineering and computer science from University of Michigan, Ann Arbor, in April 2002. He is currently working toward the Ph.D. degree in electrical engineering and computer science at the University of Michigan.

His research work at the University of Michigan focused on integrated DNA analysis systems employing solid-state, surface-micromachined

porous-plug electroosmotic pumps and thermally responsive polymer valves both of which require development of micromachining techniques for novel polymer films.



Sam Miller received the Ph.D. degree in solid-state physics from Iowa State University, Ames, in 1984, where he investigated superconducting tunneling phenomena.

He then joined Sandia National Laboratories, Albuquerque, NM, where he worked for 16 years. While at Sandia National Laboratories, he made fundamental contributions in the areas of semiconductor technology, device physics, and predictive reliability, directly resulting in fielded products in space and weapons applications. He also made fundamental contributions to the development of Sandia's MEMS program, particularly in the areas of MEMS device physics, reliability, and design. In 2000, he left Sandia and co-founded MEMX, a MEMS product development company. He is an inventor of over 25 patents pending or issued, and has authored or coauthored well over 50 technical publications.



Katsuo Kurabayashi (M'00) received the B.S. degree in precision machinery engineering from the University of Tokyo, Japan, in 1992 and the M.S. and Ph.D. degrees in materials science and engineering with electrical engineering minor from Stanford University, Stanford, CA, in 1994 and 1998, respectively. His dissertation work focused on measurement and modeling of the thermal transport properties of electronic packaging and organic materials for integrated circuits under the contract with the Semiconductor Research Corporation (SRC).

Upon completion of his Ph.D. program, he was hired as Research Associate with the Department of Mechanical Engineering at Stanford University for 12 months. In January 2000, he joined the University of Michigan, Ann Arbor, where he is an Assistant Professor with the Department of Mechanical Engineering. At the University of Michigan, he mentors five doctoral students who are investigating thermal transport phenomena in MEMS structures and electronic devices, novel actuator and micromechanism designs for MEMS optical detection devices, and multiphysics modeling and characterization of RF MEMS.

Dr. Kurabayashi is a recipient of the 2001 NSF CAREER Award and is a Member of the American Society of Mechanical Engineers (ASME).



James J. Allen received the B.S. and M.S. degrees in mechanical engineering from the University of Arkansas in 1971 and 1977, respectively. He received the Ph.D. degree in mechanical engineering from Purdue University, West Lafayette, IN, in 1981.

He is a registered professional engineer in the state of New Mexico and has spent six years in the U.S. Navy nuclear propulsion program and served aboard fast attack submarines. Currently, he is a member of the MEMS Device Technology Department at Sandia National Laboratories, Albuquerque, NM, where he has worked for 18 years and holds three patents for MEMS devices.

Dr. Allen is a Member of the American Society of Mechanical Engineers (ASME).